Heliyon 10 (2024) e27597

Contents lists available at ScienceDirect

Heliyon

journal homepage: www.cell.com/heliyon

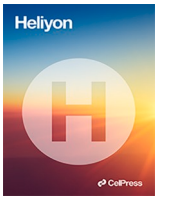

Research article

Integration of 16S rRNA sequencing and metabolomics to investigate the modulatory effect of ginsenoside Rb1 on atherosclerosis

Yuqin Liang, Jiaqi Fu, Yunhe Shi, Xin Jiang, Fang Lu **, Shumin Liu *

Institute of Traditional Chinese Medicine, Heilongjiang University of Chinese Medicine, Harbin, 150040, China

ARTICLE INFO

Keywords:
Atherosclerosis
Ginsenoside Rb1
Inflammation
Gut microbiota
Short-chain fatty acid
Metabolomics

ABSTRACT

Background: /aims: Atherosclerosis (AS) is the common pathological basis of a variety of cardiovascular diseases (CVD), and has become the main cause of human death worldwide, and the incidence is increasing and younger trend. Ginsenoside Rb1 (Rb1), an important monomer component of the traditional Chinese herb ginseng, known for its ability to improve blood lipid disorders and anti-inflammatory. In addition, Rb1 was proved to be an effective treatment for AS. However, the effect of Rb1 on AS remains to be elucidated. The aim of this study was to investigate the mechanisms of Rb1 in ameliorating AS induced by high-fat diet (HFD).

Materials and methods: In this study, we developed an experimental AS model in Sprague-Dawley rats by feeding HFD with intraperitoneal injection of vitamin D3. The potential therapeutic mechanism of Rb1 in AS rats was investigated by detecting the expression of inflammatory factors, microbiome 16S rRNA gene sequencing, short-chain fatty acids (SCFAs) targeted metabolomics and untargeted metabolomics.

Results: Rb1 could effectively alleviate the symptoms of AS and suppress the overexpression of inflammation-related factors. Meanwhile, Rb1 altered gut microbial composition and concentration of SCFAs characterized by Bacteroidetes, Actinobacteria, Lactobacillus, Prevotella, Oscillospira enrichment and Desulfovibrio depletion, accompanied by increased production of acetic acid and propionic acid. Moreover, untargeted metabolomics showed that Rb1 considerably improved faecal metabolite profiles, particularly arachidonic acid metabolism and primary bile acid biosynthesis.

Conclusion: Rb1 ameliorated the HFD-induced AS, and the mechanism is related to improving intestinal metabolic homeostasis and inhibiting systemic inflammation by regulating gut microbiota.

1. Introduction

Cardiovascular disease (CVD) is the leading cause of chronic disability and premature mortality worldwide, which seriously threatens people's health [1]. Atherosclerosis (AS) is a chronic inflammatory disease occurring in the endarterium, which can induce a variety of acute cardiovascular and cerebrovascular events, including coronary heart disease, myocardial infarction, stroke [2]. The

* Corresponding author.
** Corresponding author.
E-mail addresses: lufang_1004@163.com (F. Lu), shumliu0321@163.com (S. Liu).

https://doi.org/10.1016/j.heliyon.2024.e27597
Received 14 November 2023; Received in revised form 4 March 2024; Accepted 4 March 2024
Available online 5 March 2024

pathological characteristics of the disease are disorders of lipid metabolism, endothelial cell damage, macrophage aggregation and aberrant proliferation of vascular smooth muscle cells [3]. The risk factors for AS are increasing globally, mainly due to hyperlipidemia, diabetes mellitus, microbiome, smoking and air pollution [4,5]. At present, the treatment of AS mainly focuses on lipid-lowering and antithrombotic therapy, such as lipid-lowering agent statins and anti-platelet agent aspirin [6]. However, these methods have limitations in clinical application and might produce serious adverse reactions. Therefore, it is necessary to develop more drugs with lower toxicity and greater efficacy to expand the clinical drug options.

The gut microbiota (GM) has been described as the "second genome" of humans, intervening in numerous physiological processes, including energy metabolism, digestion and absorption, immune inflammation and the formation of intestinal mucosal barriers [7–9]. The GM dysbiosis can influence the onset and progression of numerous CVDs [10,11]. GM-artery axis refers to the bidirectional pathway between GM and its metabolites and the cardiovascular system [12]. It is believed that the disorder of GM-artery axis is critical pathogenic factors of AS, which is characterized by lipid metabolism disorder, activation of the inflammatory response, bacterial structure imbalance and low short-chain fatty acids (SCFAs) production [13–15]. SCFAs alleviates AS through a variety of pathways, including regulating lipid metabolism, inhibiting the expression of inflammatory factors and vascular adhesion molecules and improving endothelial function [16,17]. Thus, targeting GM may provide a new strategy for the prevention and treatment of AS.

Traditional Chinese medicine (TCM) and their derived natural compounds have attracted increasing attention in clinical management of AS due to the advantages of extensive pharmacological activities, low adverse reactions and significant therapeutic effects synergies [18,19]. As one of the traditional precious Chinese medicinal materials, ginseng has the effect of invigorating the vitality, tranquilizing the mind, strengthening the brain, which is suitable for the atherosclerotic pathogenesis of "qi deficiency and blood stasis" in the modern TCM theory. Ginsenosides are the main pharmacologically active components of ginseng. Among them, Rb1 is a key panaxadiol saponin isolated from the stem, root and flower buds of ginseng. Pharmacological and clinical studies have confirmed the remarkable efficacy of Rb1 in the treatment of AS and AS-associated CVDs [20–22]. In vivo experiments Rb1 exhibits preventive and therapeutic effects on atherosclerosis by enhancing autophagy [23]. In vitro experiments, Rb1 synergistically regulates Keap1 and $p47^{phox}$ in endothelial cells, thereby ameliorating endothelial cell injury by promoting Nrf2 activation under oxidative stress [24]. In addition, several studies have demonstrated that RB1 ameliorates vascular smooth muscle injury through multiple mechanisms [25–27]. However, the exact mechanism of Rb1 against AS still requires further study.

In the present study, we demonstrated that Rb1 regulates lipids and inhibits inflammation in favor of AS treatment. Then, the potential mechanism of Rb1 in the treatment of AS rats was investigated by integrating microbiome 16S rRNA gene sequencing, SCFAs targeted metabolomics and untargeted metabolomics. The research approach is shown in Fig. 1.

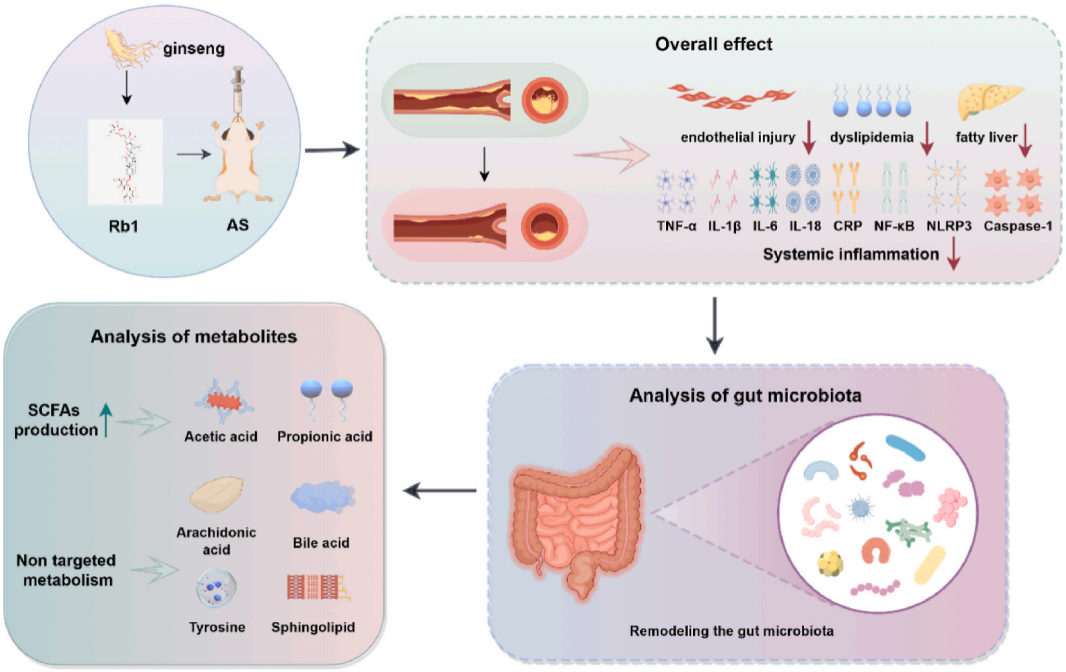

Fig. 1. Graphical abstract of full-text experiments.

2. Materials and methods

2.1. Animals

A total of Fifty SPF-grade male Sprague-Dawley rats with body weights between 180 and 220g were purchased from Liaoning Changsheng Biotechnology Co. Ltd., Liaoning, China (Certificate of Conformity: SCXK (Liao) 2020–0001). They were raised in the Institute of Chinese Medicine Research, Heilongjiang University of Chinese Medicine (onstant temperature of 24 ± 2 °C, 12 h light/dark cycle). The animal study protocol was approved by the Animal Ethics Committee of Heilongjiang University of Chinese Medicine (Ethics number: No. 2022062023).

2.2. Materials and reagents

Rb1 (B21050) were obtained from the Shanghai yuanye Bio-Technology Co., Ltd. (Shanghai, China). Atorvastatin calcium tablets (Ato, H20051408) purchased from Pfizer Inc. (New York, USA). HFD is compressed according to basic feed +10% lard +10% egg yolk powder +1.25% cholesterol +0.5% sodium cholate, provided by the Xiaoshuyoutai Biotechnology Co., Ltd (Beijing, China). The following assay kits were obtained from Nanjing Jiancheng Bioengineering Institute (Nanjing, China): Triglyceride (TG, A110-1-1), Total Cholesterol (TC, A111-1-1), Low-density lipoprotein cholesterol (LDL-C, A113-1-1), High-density lipoprotein cholesterol (HDL-C, A112-1-1), Interleukin-1β (IL-1β, H002-1-2), IL-6 (H007-1-2), IL-18 (H015-1-2), C-reactiveprotein (CRP, H126-1-2) and tumor necrosis factor-α (TNF-α, H052-1-2). The following antibodies were provided from Servicebio Biotechnology Co., Ltd (Wuhan, China): NLRP3 (GB114320), Caspase-1 (GB11383), NF-κB p65 (GB11997), GAPDH (GB15004) and HRP conjugated Goat Anti-Rabbit IgG (GB23303). The following reagents were provided from Servicebio Biotechnology Co. Ltd (Wuhan, China): BCA Protein Assay Kit (G2026), Protein-free rapid blocking solution (G2052). SDS-PAGE Loading Buffer (G2013).

2.3. Experiment grouping and AS model establishment

After adaptively fed for 1 week, fifty rats were randomly divided into five groups as follows (n = 10): blank control group (BC), AS model group (AS), Rb1-treated group (LD-10 mg/kg, HD-20 mg/kg) and Ato-treated group (Ato-1.8 mg/kg). Except BC group, and the remaining 50 rats were injected once intraperitoneally with vitamin D3 (600,000 IU/kg) and then HFD-fed for 8 weeks to induce the AS model [28]. Starting from the 9th week, the rats in each group were intragastric administration of the corresponding drug or distilled water, once a day for 4 weeks. After 4 weeks of treatment, all rats were deeply anesthetized with 30 mg/kg pentobarbital sodium and sacrificed. Blood, thoracic aorta, liver, and cecal contents were collected quickly.

2.4. Pathological assessment of thoracic aorta and liver

The thoracic aorta and liver were fixed in 4% paraformaldehyde fixative for 72 h and embedded with paraffi. The sections were successively sliced with a thickness of 4 μm, followed by xylene transparency, gradient ethanol dewaxing and hydration. Hematoxylin-eosin (HE) staining was performed according to the instructions of the kit, and histopathological changes of the thoracic aorta were observed by light microscope (magnification × 200).

2.5. Serum lipids detection

Blood samples were centrifuged at 3000 rpm for 10 min and the serum was collected. The TG, TC, LDL-C, HDL-C levels of rat serum were used to evaluate the dyslipidemia, and the TG, TC, LDL-, HDL-C levels of rat serum were measured with an automatic biochemical analyzer according to the operating instructions of the kits.

2.6. Serum inflammatory factor detection

The IL-1β, IL-6, IL-18, CRP and TNF-α levels of rat serum were used to evaluate the assess the progression of inflammation, and the concentration of serum IL-1β, IL-6, IL-18, CRP and TNF-α in each group of rats were detected by ELISA kits, strictly in accordance with manufacturer's instructions.

2.7. Western blot analysis

Proteins of treated thoracic aorta homogenates was extracted following standard protocols, and the protein concentration was measured using the BCA protein assay kits. Equal amounts of protein samples were separated on 10% SDS-PAGE gel (tacking gel 100 V for 30min, separating gel 120 V for 1 h) and transferred onto PVDF membranes. The membranes were blocked in fast blocking materials for 5 min and incubated with the diluted primary antibodies NLRP3 (1:1000), Caspase-1 (1:1000), NF-κB p65 (1:1000) and GAPDH (1:2000) overnight at 4 °C. The membranes were washed three times with TBST and incubated with secondary antibodies (1:3000) for 1 h at room temperature. Finally, the membranes were visualized using the CLINX 6100 imaging system and the bands were quantified using Image J software.

2.8. Microbiome 16S rRNA gene analysis

The total DNA of rat stool samples were extracted with the DNA extraction kit. PCR amplification of the V3–V4 variable region of the 16S rDNA gene and sequenced by the HiSeq 2500 System at the Paired-end. The raw sequence fastq files were denoised, spliced and chimeras removed in the QIIME2 platform to obtain the ASV (amplicon sequence variants) feature sequence table. The community composition analysis, α-diversity analysis, β-diversity analysis and differential species analysis were performed with QIIME2 platform to identify the alterations in the GM. The raw sequence reads are available in SRA with the accession number (PRJNA950603).

2.9. Determination of SCFAs in cecal contents

The fecal test samples were prepared according to Yan's [29] method, and the concentration levels of acetic acid, propionic acid, butyric acid, isobutyric acid, pentanoic acid, isovaleric acid and hexanoic acid in feces were determined by gas chromatography in combination with mass spectrometry (GC–MS). The concentration of SCFAs were calculated by detecting different concentrations of standard mixtures and plotting the standard curve with the peak area as the abscissa and the standard concentration as the ordinate. The chromatographic conditions were as follows: The analysis was performed on an Agilent J&W DB-FFAP (30 m × 0.25 mm, 0.25 μm) column; Helium with purity ≥99% was selected as the carrier gas with the constant flow rate of 1.2 mL/min; The sampling volume was 1 μL with shunt ratio of 10:1; The temperature program: 0–3 min, 80–120 °C; 3~7min; 120–200 °C; 7~9min, 200–230 °C; 9~14min, 230 °C. The mass spectrometry conditions were as follows: electron impact ion source with the electron energy of 70 eV; The temperatures of the transmission line, EI ion source and quadrupole are 290 °C, 230 °C, and 150 °C, respectively; The scanning range of sample acquisition: 30–300 *m/z*.

2.10. Untargeted metabolomic analysis

Weigh 60 mg fecal sample and then mixed with 540 μL pre-cooled extraction solution (methanol: water = 3:1, v/v). After grinding treatment at 40 Hz for 3 min, an ultrasound was carried out in ice water for 10 min. Then, centrifuge at 4 °C, 12,000 rpm for 15 min, and take the supernatant into the sample bottle for machine test. Chromatographic conditions: A Waters ACQUITY UPLC HSS T3 (2.1 mm × 100 mm, 1.8 μm) column maintained at 40 °C. Mobile phase: A-water (contains 25 mM ammonium acetate and 25 mM ammonia

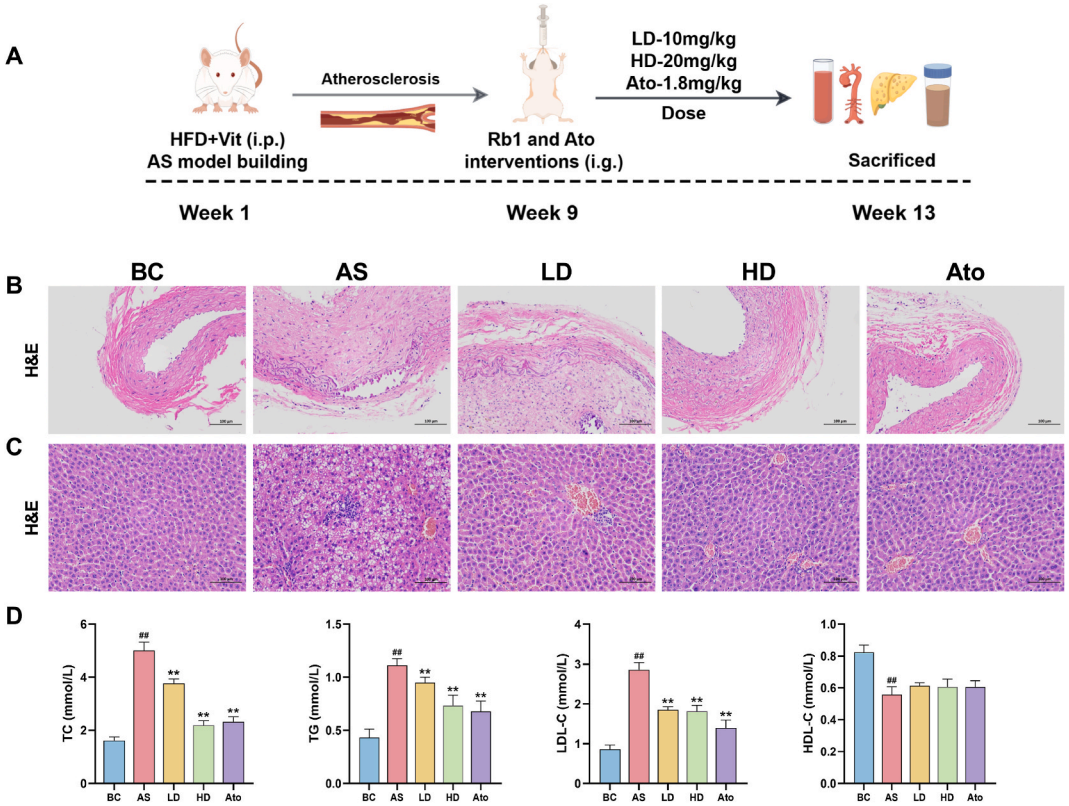

Fig. 2. Effects of Rb1 on AS rats. (A) Experimental protocol for the treatment of AS rats by Rb1. (B) HE staining of thoracic aorta, Scale bars = 100 μm (n = 4). (C) HE staining of liver tissue, Scale bars = 100 μm (n = 4). (D) blood lipid levels. Results were expressed as mean ± SD (n = 8). (#p < 0.05, ##p < 0.01 vs the BC. *p < 0.05, **p < 0.01 vs the AS).

water), B-acetonitrile. The gradient program: 0~0.5 min, 95% B; 0.5–5 min, 95%–65% B; 5–9 min, 65%–46% B; 9~9.5 min, 46%–95% B; 9.5–12 min, 95% B. Flow rate: 0.4 mL/min. Autosampler temperature: 4 °C. sampling volume: 3 μL.

2.11. Statistical analysis

GraphPad Prism 9.5 and SPSS 22.0 software were used for image production and statistical analysis, and the data results were shown as mean ± standard deviation (SD). One-way ANOVA was used to compare the differences between groups. Microbiome 16S rRNA sequencing and metabolomics results were analyzed by Kruskal - Wallis test. Correlation analysis was performed by Spearman's correlation coefficient.

3. Results

3.1. Pathological observation of aortic tissue

The buildup of plaque and inflammatory infiltration are the pathological characteristics of the aorta in AS rats. Compared with the BC group, the aortic tissue cell structure was obvious impaired in the AS group, with calcium salt deposition, fibrous plaque formation, intima damage and inflammatory infiltration. After administration, the aorta AS-related pathological morphology was improved to varying degrees in all groups, mainly manifested as normal smooth muscle cell morphology, reduced inflammatory infiltration and calcium salt deposition, and improved endothelial damage, especially in HD and Ato groups (Fig. 2-B).

3.2. Pathological observation of liver tissue

The existence and severity of NAFLD are closely related to the development of AS. Compared with the BC group, a large number of liver cell steatosis, loose cytoplasm, and multiple round vacuoles of varying sizes were obvious observed in the liver tissue of the AS group rats. Some liver cells were swollen, and inflammatory cell infiltration was observed in multiple locations. Compared with the AS group, the intervention of each medication group conspicuously reduced the steatosis of liver cells in rat liver tissue, reduced liver cell swelling, and only a small amount of inflammatory cell infiltration was observed (Fig. 2-C).

3.3. Rb1 ameliorated HFD-induced dyslipidemia

The symptoms of HFD-induced elevated circulating concentrations of lipids are similar to the pathological manifestations of human AS. Compared with the BC, the serum levels of TC, TG and LDL were conspicuously higher in the AS group ($P < 0.05$), while the levels of HDL were conspicuously decreased ($P < 0.05$), confirming that lipid metabolism was disturbed in AS rats. After treatment, except for the TC level in the LD group, the serum levels of TC, TG and LDL in each dosing groups were conspicuously decreased ($P < 0.05$). However, there was no significant in serum HDL levels among each administration groups (Fig. 2-D).

3.4. Rb1 regulated the level of inflammatory cytokines in AS rats

Inflammation is an essential pathogenetic driver of AS, directly involved in the whole course of AS [30]. Adverse changes of GM and its metabolites can enhance systemic inflammation to promote the progression of AS [31]. Therefore, we examined the expression contents of inflammatory cytokines in serum and aortic tissue. The levels of inflammatory cytokines including TNF-α, IL-1β, IL-6, IL-18

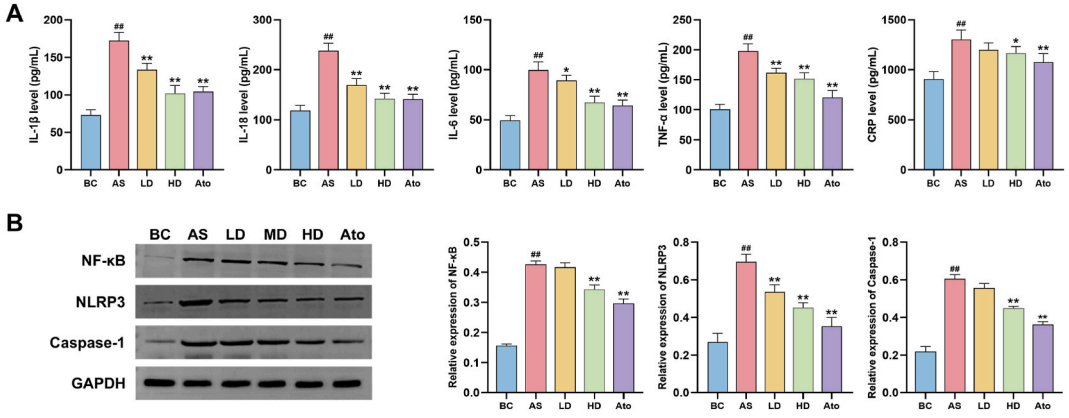

Fig. 3. Rb1 Inhibited inflammation in AS rats. (A) Serum TNF-α, IL-1β, IL-6, IL-18 and CRP were detected by ELISA kit (n = 8). (B) Expression of NF-κB, NLRP3 and Caspase-1 in thoracic aorta detected by Western blot. Results were expressed as mean ± SD (n = 4). (#$p < 0.05$, ##$p < 0.01$ vs the BC. *$p < 0.05$, **$p < 0.01$ vs the AS).

and CRP in serum were conspicuously increased in AS group compared with the BC group ($P < 0.05$). After Rb1 treatment, the abnormal increases in the levels of five inflammatory cytokines were reduced in a dose-dependent manner. Compared with the AS group, the concentrations of IL-1β, TNF-α, IL-6 and IL-18 in group LD, HD and Ato were conspicuously decreased ($P < 0.05$). In addition, the concentrations of CRP were conspicuously decreased in group HD and Ato ($P < 0.05$) (Fig. 3-A).

The protein expressions of NF-κB, NLRP3 and Caspase-1 were conspicuously increased in AS group compared with the BC group ($P < 0.05$). With the administration of Rb1, the protein expressions of NF-κB and Caspase-1 in group HD and Ato were conspicuously decreased, and the protein expressions of NLRP3 were conspicuously decreased in each administration groups ($P < 0.05$) (Fig. 3-B).

3.5. Rb1normalized the GM composition in AS rats

Through the above pharmacodynamic study, it was confirmed that the anti-AS effect of high-dose Rb1 was the best, thus the fecal samples from BC, AS and HD groups were selected for high-throughput sequencing to investigate the effect of Rb1 administration on the GM composition. After completing quality-filtering, de-noising, splicing and chimera removal, a total of 1,430,658 high quality sequences were generated. The rarefaction curves and rank-abundance curve constructed after OTU clustering indicated that the sequencing depth of samples was sufficient to reflect the microbial diversity information of samples and the species composition was homogeneous (Fig. 4-A).

Alpha-diversity indices, including chao1, observed species, shannon and simpson index were analyzed to estimate diversity and richness of species. We observed that chao1, observed species and shannon diversity index were conspicuously reduced and Simpson Diversity index was conspicuously increased in the AS group compared with the BC group ($P < 0.05$). After intervention with Rb1, chao1 and shannon diversity index were conspicuously increased compared with the AS group ($P < 0.05$). However, Rb1 had no obvious effect on observed species and simpson index ($P > 0.05$) (Fig. 4-B).

We explored species similarity or differences of microbial communities in beta diversity, including PCoA and NMDS. The samples of

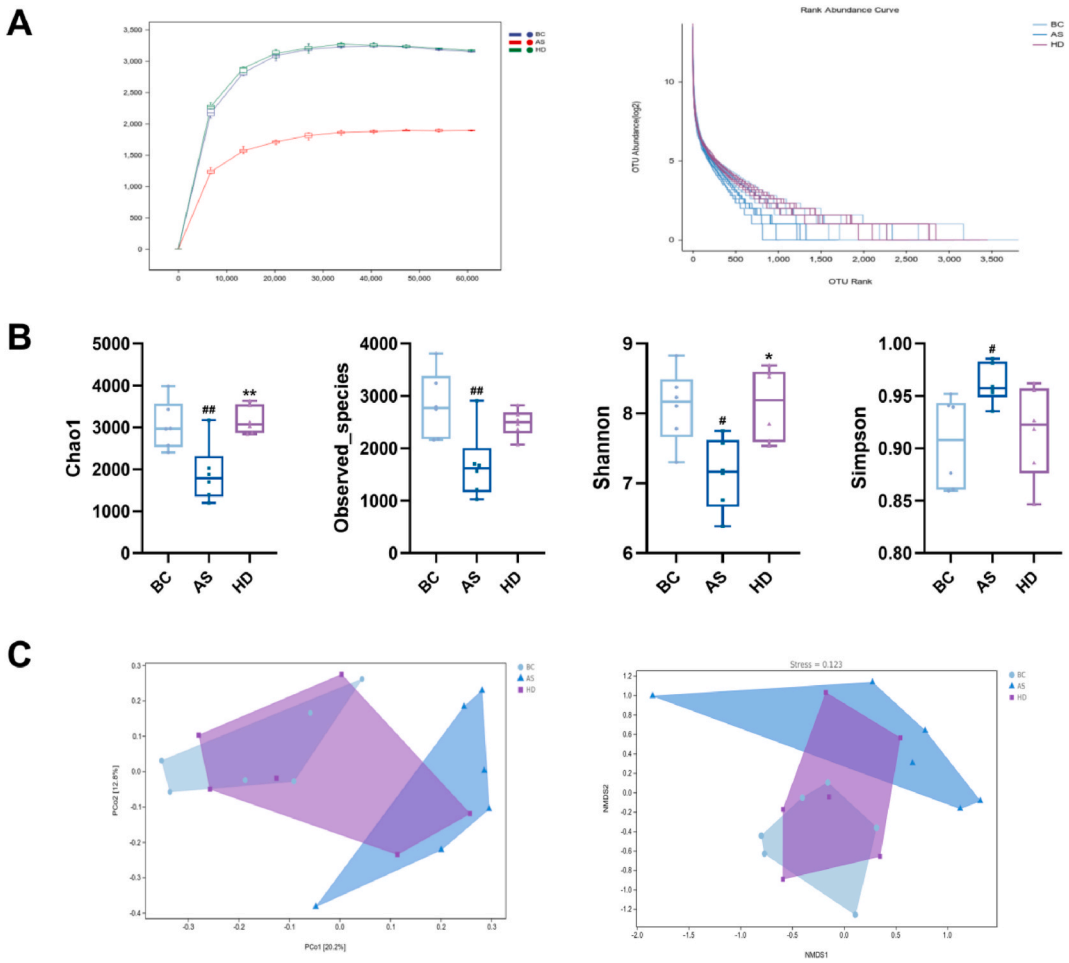

Fig. 4. The results of microbial diversity analysis. (A) rarefaction curve and rank abundance curv. (B) α-Diversity. (C) β-diversity. Results were expressed as mean ± SD (n = 6). (#p < 0.05, ##p < 0.01 vs the BC. *p < 0.05, **p < 0.01 vs the AS).

BC group and AS group were obviously separated, which indicated that the GM of AS model rats had obvious variation. After the intervention of Rb1, the distribution of GM tended to migrate to the BC group, which indicated that Rb1 had a certain regulatory effect on the composition of GM community in AS rats (Fig. 4-C).

At the phylum level, the predominant GM of each group is Firmicutes and Bacteroidetes, followed by Proteobacteria, Actinobacteria and Tenericutes. The proportion of Bacteroidetes and Actinobacteria were conspicuously decreased in AS group compared with the BC group ($P < 0.05$), while the proportion of Firmicutes and Firmicutes/Bacteroidetes (F/B) increased conspicuously ($P < 0.05$). Rb1-treatment led to a significant increase in the abundance of Bacteroidetes and Actinobacteria ($P < 0.05$). After Rb1 intervention, the proportion of Bacteroidetes and Actinobacteria were conspicuously increased ($P < 0.05$) and the proportion of F/B was conspicuously decreased ($P < 0.05$). In contrast, the proportion of Firmicutes and Proteobacteria showed a decreasing trend, but the difference was not obvious (Fig. 5-A). At the genus level, the first five representative dominant bacteria related to AS were Lactobacillus, Prevotella, Oscillospira, Blautia and Desulfovibrio. AS modelling increased the abundance of Desulfovibrio, while suppressed

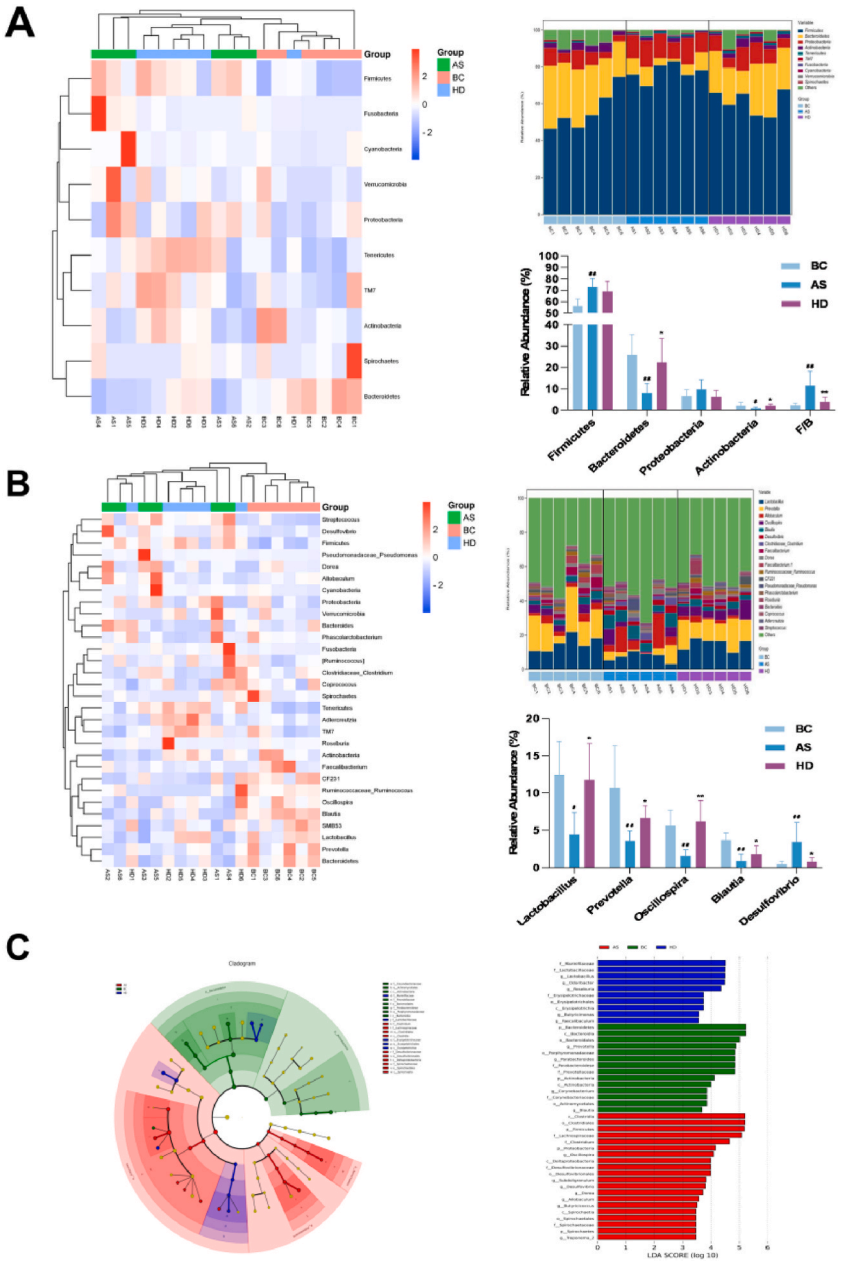

Fig. 5. Rb1 reshaped the GM in AS rats. (A) Bacterial taxonomic profiling and differential bacteria at the phylum level. (B) Bacterial taxonomic profiling and differential bacteria at the genus level. (C) LDA value distribution histogram and species bifurcation evolution diagram. Results were expressed as mean ± SD (n = 6). (#$p < 0.05$, ##$p < 0.01$ vs the BC. *$p < 0.05$, **$p < 0.01$ vs the AS).

the abundance of Lactobacillus, Prevotella, Oscillospira and Blautia ($P < 0.05$). Rb1 treatment reversed the changes in Lactobacillus, Prevotella and Oscillospira and Desulfovibrio abundance ($P < 0.05$) (Fig. 5-B).

Linear discriminant analysis effect size (LEfSs) was used to determine the GM associated with Rb1 treatment. There were 14 species with conspicuous difference in the BC group, mainly including Bacteroidetes, Prevotellaceae, Porphyromonadaceae and Actinobacteria. There were 20 species with conspicuous difference in the AS group, mainly including Clostridia, Lachnospiraceae, Firmicutes, Desulfovibrionaceae. There were 10 species with conspicuous difference in the HD group, mainly including Marinifilaceae, Lactobacillales and Odoribacter (Fig. 5-C).

3.6. Rb1 promoted the SCFAs production in AS rats

Given the protective role of SCFAs in the pathogenesis of AS, we conducted a quantitative analysis of the concentrations of SCFAs in feces, including acetic acid, propionic acid, butyric acid, isobutyric acid, pentanoic acid, isovaleric acid and hexanoic acid. AS modelling considerably reduced the concentrations of acetic acid, propionic acid and butyric acid ($P < 0.05$). Rb1 administration markedly increased the acetic acid, propionic acid production ($P < 0.05$), butyric acid production tended to be upregulated but not significant (Fig. 6-A, B).

3.7. Metabonomic analysis

The PCA scoring diagram (Fig. 7-A, D) in positive and negative ion modes showed that the BC and AS group were separated along the t1 axis and there was obvious separation, indicating that AS modelling interfered with normal metabolism of rats. After Rb1 intervention, there were obvious differences in metabolic profiles between Rb1 group and AS group, indicating that they had significantly different metabolic characteristics. To further verify the changes of endogenous metabolites in AS rats after Rb1 administration, supervised PLS-DA (Fig. 7-B, E) analysis was performed, which can achieve better intergroup separation than PCA. The results showed that fecal metabolic profiles of the three groups of rats achieved good clustering, reflecting that the metabolic profiles can effectively distinguish the separation trend of rats in the group AS and the BC, indicating that the fecal metabolome can be scientifically and effectively applied to the judgment of pathological and physiological states.

VIP$\geq$1, FC $\geq$ 1.2 and $P < 0.05$ were selected as the screening criteria for potential variables in positive and negative ion modes (Fig. 7-C, F). The secondary spectra of the obtained variables were identified with the HMDB database to finally screen out the potential differential metabolites. A total of 45 metabolites were identified in feces. We performed cluster analysis of 45 differential metabolites among the group BC, AS and HD (Fig. 7-G). According to the results, there were substantial changes in the levels of metabolites in AS rats induced by HFD, with 10 and 29 metabolites markedly downregulated and upregulated, respectively. However, the Rb1 intervention substantially regulated 30 metabolites and eliminated changes in 25 metabolites. The 45 selected metabolites (Table 1) were imported into Metabo Analyst 5.0 database for potential metabolic pathway analysis. The top five pathways with the highest activity were mainly enriched in Arachidonic acid metabolism, Primary bile acid biosynthesis, Tyrosine metabolism, Sphingolipid metabolism and Lysine degradation (Fig. 7-H, I).

3.8. Correlation analysis

Spearman correlation analysis was used to investigate the correlation between GM and their differential metabolites and inflammatory cytokines. In the differential GM, we found that Bacteroidetes, Lactobacillus, Prevotella, Oscillospira and Blautia have a strong negative correlation with various pro-inflammatory cytokines, while Desulfovibrio and Firmicutes have an obvious positive correlation with various pro-inflammatory cytokines (Fig. 8-A, B). Rb1-promoted production of acetic acid and propionic acid showed a strong negative correlation with AS-associated pro-inflammatory factors, suggesting that Rb1 might inhibit inflammation in AS rats

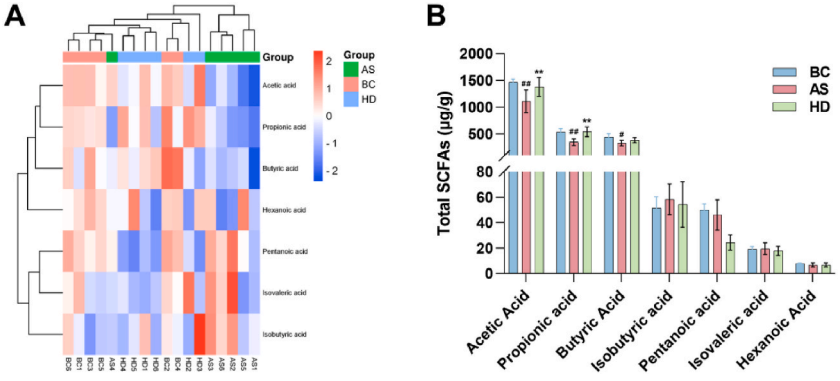

Fig. 6. Effects of Rb1 on SCFAs in cecal contents of the AS rats. (A) Heatmap of SCFAS concentrations. (B) Analysis of differences in SCFAs concentrations among groups. Results were expressed as mean ± SD (n = 6). (#$p < 0.05$, ##$p < 0.01$ vs the BC. *$p < 0.05$, **$p < 0.01$ vs the AS).

Table 1
List of screened differential metabolites.

No.	Ion mode	Metabolites	Formula	ppm	FC	AS/BC Trend	p	HD/AS Trend	P
1	–	Murocholic acid	C24H40O4	−0.820293632	3.107583661	↑	**	↓	**
2	–	Lithocholic acid	C24H40O3	−0.847061762	17.16995553	↑	**	↓	**
3	–	15-Keto-prostaglandin E2	C20H30O5	−1.119710727	2.845610323	↑	**	↓	–
4	–	Prostaglandin E2	C20H32O5	−2.223958205	1.89097295	↑	*	↓	–
5	–	Taurochenodesoxycholic acid	C26H45NO6S	−3.046594176	5.306209201	↑	**	↓	**
6	–	Allocholic acid	C24H40O5	0.079055248	25.28497674	↑	**	↓	**
7	–	Hepoxilin A3	C20H32O4	−1.055460444	3.437799633	↑	–	↓	**
8	–	15-Deoxy-d-12,14-PGJ2	C20H28O3	−1.564322694	2.373741104	↑	**	↓	–
9	–	Isoursodeoxycholic acid	C24H40O4	−0.599371483	2.59107211	↑	**	↓	**
10	–	SM(d18:1/12:0)	C35H71N2O6P	−3.587255504	2.029616566	↓	**	↑	**
11	–	Galactosylsphingosine	C24H47NO7	−17.86049383	3.610884873	↑	**	↓	**
12	–	19-Hydroxytestosterone	C19H28O3	−0.524035269	4.091905646	↑	*	↑	–
13	–	20-Hydroxyeicosatetraenoic acid	C20H32O3	−0.722969983	3.063126921	↑	*	↑	–
14	–	Kynurenic acid	C10H7NO3	−3.888416197	3.7824209	↓	**	↑	–
15	–	5-Hydroxy-L-tryptophan	C11H12N2O3	−37.08630571	5.361104994	↑	–	↑	**
16	–	Taurocholic acid	C26H45NO7S	5.975173831	2.275336637	↑	**	↓	–
17	–	Cholic acid	C24H40O5	−0.185829536	4.796003561	↑	**	↓	**
18	–	Leukotriene D4	C25H40N2O6S	−2.333147097	2.637097118	↑	**	↓	**
19	–	Homogentisic acid	C8H8O4	−17.86482122	1.579196329	↓	–	↓	**
20	–	Corticosterone	C21H30O4	−0.527486996	43.16246081	↑	**	↑	**
21	–	L-Urobilin	C33H46N4O6	−7.00339739	14.90083047	↓	**	↓	–
22	–	Indole	C8H7N	−6.29520464	2.356277031	↓	**	↓	–
23	–	Inosine	C10H12N4O5	−2.625599462	1.938826732	↓	**	↓	–
24	–	Uridine	C9H12N2O6	−3.959560589	2.024075698	↓	*	↓	**
25	–	Gentisate aldehyde	C7H6O3	−6.143831501	7.918824414	↓	**	↑	**
26	–	5-Acetamidovalerate	C7H13NO3	−3.92752738	9.20755571	↑	–	↑	**
27	–	Sphingosine 1-phosphate	C18H38NO5P	0.305192471	10.23461223	↑	**	↓	**
28	+	Cholesterol	C27H46O	−18.26591201	3.280647762	↑	*	↓	–
29	+	Docosapentaenoic acid	C22H34O2	−24.19146813	3.188251077	↑	*	↓	**
30	+	Barbituric acid	C4H4N2O3	102.996137	2.383543652	↑	**	↓	**
31	+	19(S)-HETE	C20H32O3	−28.12311832	2.071204716	↓	**	↑	–
32	+	Alpha-Linolenic acid	C18H30O2	−24.09816048	2.237663739	↑	**	↓	*
33	+	Deoxycholic acid	C24H40O4	−14.03334074	2.86159394	↑	**	↓	**
34	+	Traumatic acid	C12H20O4	15.90464797	5.116822202	↑	**	↓	**
35	+	Aminoadipic acid	C6H11NO4	−48.26707338	2.094902821	↑	**	↓	**
36	+	Alpha-Muricholic acid	C24H40O5	−10.78805359	55.88666321	↑	**	↓	**
37	+	Ursocholic acid	C24H40O5	−14.48256683	4.558307616	↑	**	↓	**
38	+	Troxilin B3	C20H34O5	20.68415602	14.05992153	↑	**	↓	–
39	+	Thromboxane B2	C20H34O6	16.39424663	3.78920567	↑	**	↓	–
40	+	9,12,13-TriHOME	C18H34O5	−15.92124044	3.348520992	↓	–	↑	**
41	+	Imidazole acetol-phosphate	C6H9N2O5P	4.522298627	23.37689722	↓	*	↑	**
42	+	Lithocholate 3-O-glucuronide	C30H48O9	24.35131739	3.362662313	↑	–	↓	**
43	+	Calcidiol	C27H44O2	−15.21295051	2.756127076	↑	**	↓	**
44	+	SM(d18:0/14:1 (9Z) (OH))	C37H73N2O7P	24.78197851	3.566704747	↓	**	↑	–
45	+	Saccharopine	C11H20N2O6	32.47472048	14.46541953	↑	**	↑	**

by promoting the production of SCFAs (Fig. 8-C). Furthermore, the inflammatory status is substantially related to differential metabolites. The key markers in AS inflammation were negatively correlated with differential metabolites enriched in the Arachidonic acid metabolism pathway, Primary bile acid biosynthesis pathway, Sphingolipid metabolism pathway and Lysine degradation pathway, and strongly positively correlated with differential metabolites enriched in Tyrosine metabolism pathway (Fig. 8-D).

4. Discussion

In the present study, we demonstrated that Rb1 administration attenuates arterial endothelial damage, lipid metabolism disruption and inhibits systemic inflammation in a rat model of AS. Disorders of lipid metabolism and endothelial damage are the main pathologic changes in the early stages of AS [32–34]. Dyslipidemia can induce vascular endothelial injury and regulation of macrophage phenotype, thus accelerating the formation of AS plaques [35]. In addition, we also focused on investigating the regulation of Rb1 treatment on GM and its metabolites in AS rats. Integration of metabolomics and microbiome data showed that Rb1 treatment regulated microbiota dysbiosis, promoted SCFAs production and restored related metabolites changes.

Due to inflammation is the key driver plaque formation, plaque rupture, and arterial thrombosis, it has been widely reported in AS patients and in animal models [36,37]. In the early stage of the onset, the secretion of inflammatory cytokines in the blood vessels increases, and the secretion of anti-inflammatory cytokines decreases, which results in the deposition of lipids in the vascular intima and accelerates the formation of plaques [38,39]. TNF-α and IL-6 are key inflammation-promoting cytokines in vascular inflammation

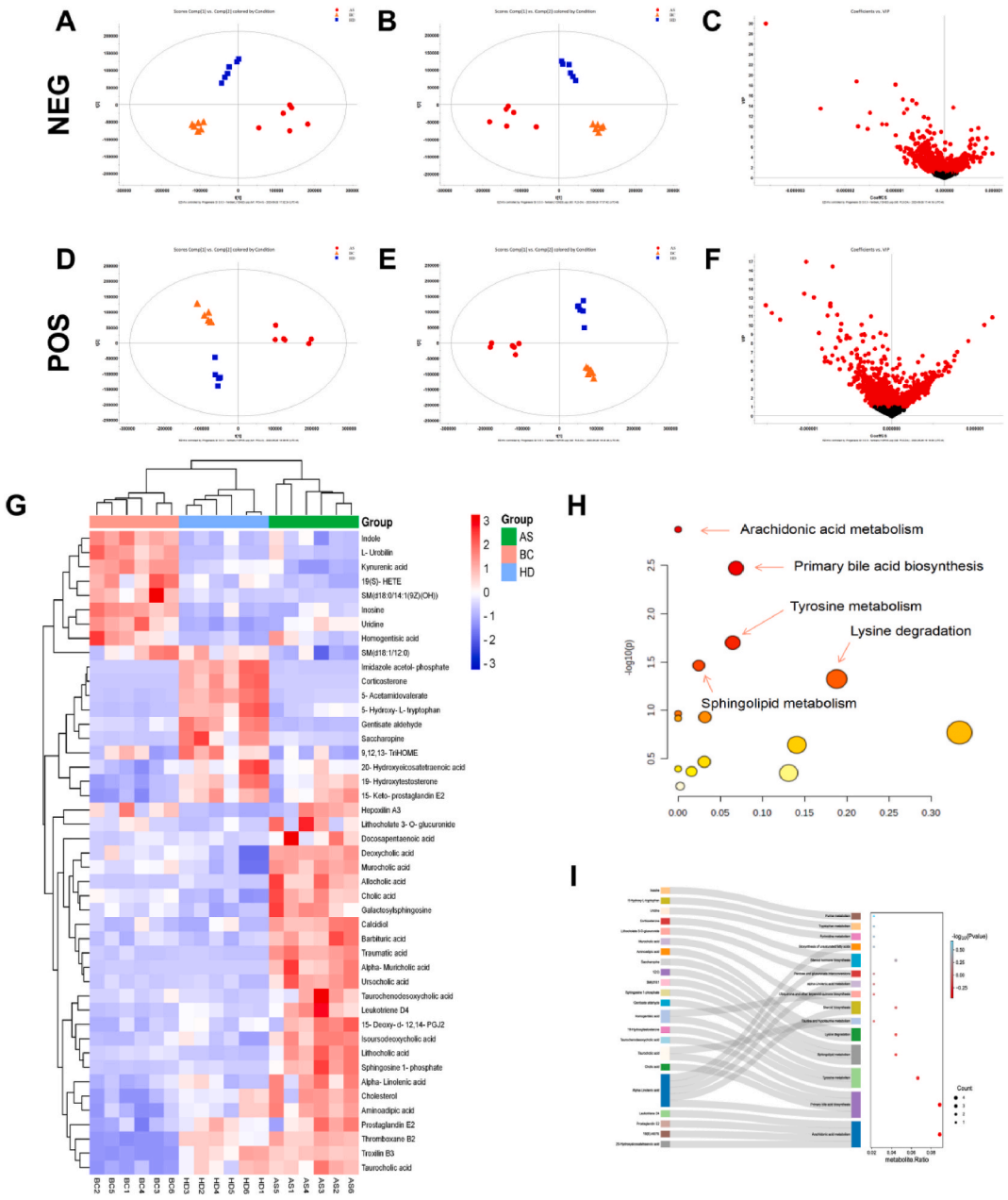

Fig. 7. Untargeted metabolic analysis of Rb1 intervention in AS rats. (A, D) PCA score plot. (B, E) PLS-DA score plot. (C, F) VIP-plot (n = 6). (G) Clustering heatmap of differential metabolites. (H, I) Metabolic pathway analysis of differential metabolites.

production and cause endothelial dysfunction [40–42]. IL-1β is primarily secreted by activated mononuclear macrophages, which is involved in various stages of vascular smooth muscle cell proliferation, macrophage activation and expression of multiple inflammatory cytokines [43,44]. As an acute inflammatory protein, CRP can promote inflammatory reaction and atherothrombosis, and is an independent predictor of CVD [45]. NF-κB, an important nuclear transcription factor in inflammation, is activated to mediate the transcription of inflammatory cytokines thereby triggering or exacerbating AS [46,47]. NLRP3 inflammasome is a multi-protein complex, which is the most widely studied inflammasome. After NLRP3 is activated, pro Caspase-1 is hydrolyzed into active Caspase-1, triggering an inflammatory response [48]. It has been shown that the mechanism of GM metabolites regulating inflammation and metabolic disorders is negatively correlated with NLRP3 activation [49]. Activated NF-κB is transferred from the cytoplasm to the nucleus and is involved in the transcriptional regulation of Caspase-1 and NLRP3, thereby inducing the production of IL-1β, IL-6 and IL-18 [50,51]. NF-κB/NLRP3 pathway reportedly influences the progression of AS by regulating inflammation and vascular plaque stability [52]. Consistent with expected results, the expression of the aforementioned proinflammatory factors was markedly elevated

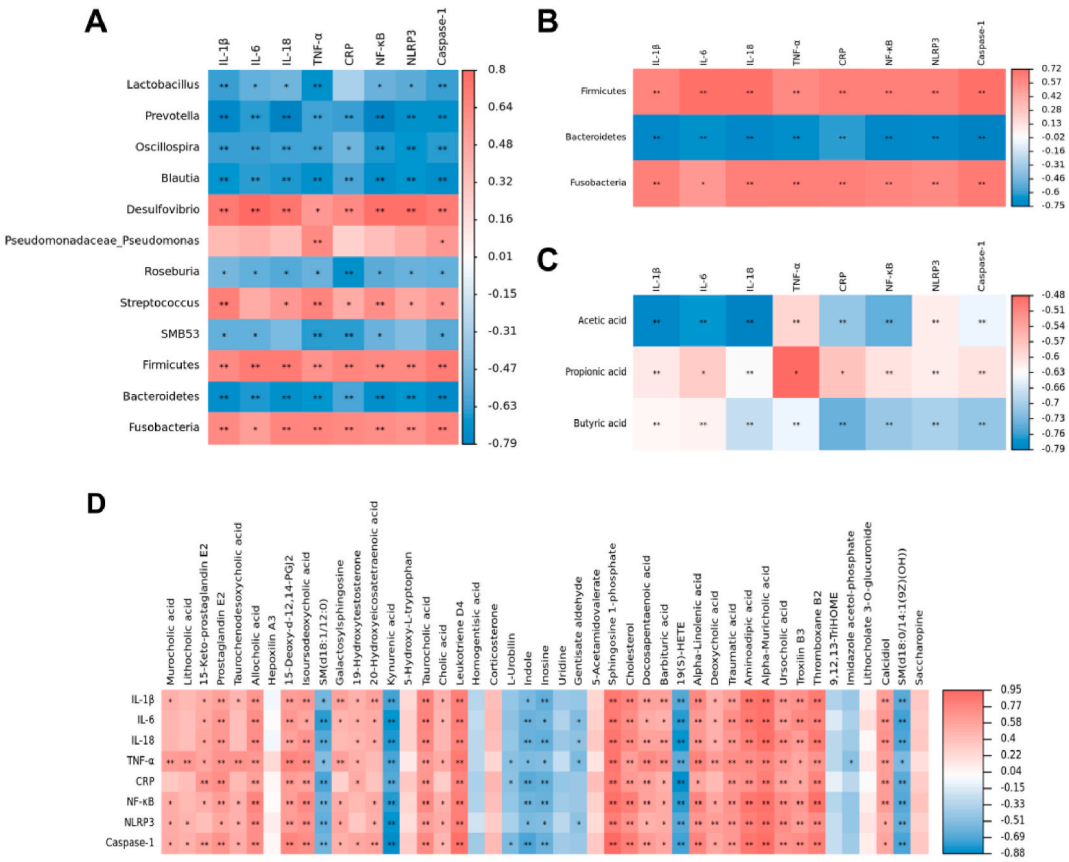

Fig. 8. Correlation analysis. (A, B) Correlation heatmap of GM (phylum and genus levels) and inflammation-related indicators levels. (C) Correlation heatmap of fecal SCFAs concentrations and inflammation-related indicators levels. (D) Correlation heatmap of differential metabolites and inflammation-related indicators levels (*p < 0.05).

in AS rats, while Rb1 treatment reversed their overexpression.

As an important part of co-evolution with the host, GM and its metabolites influence the progression of AS by affecting multiple molecular mechanisms or host genes, including modulation of macrophage infiltration, inflammatory response, lipid metabolism, and endothelial function [53–55]. Animal experiments pointed out that the intervention of probiotics or TCM can relieve the symptoms of AS patients or mice by regulating imbalance of Intestinal microenvironment [56–58]. Here, we propose a strategy to target GM and its metabolites, and further explore the mechanism of Rb1 on AS. In this study, we demonstrated that Rb1 treatment restored the microbial diversity and species richness, decreased the F/B ratio. Low alpha diversity is often used as a characteristic to evaluate dyslipidemia [59]. The increase of F/B ratio accelerated the accumulation of lipids and alters the production of SCFAs, which is a predictor of metabolic diseases [60,61]. Rb1 intervention upregulated the abundance of Lactobacillus, Prevotella and Bacteroides in AS rats. The abundance of these GM is positively correlated with the secretion of IL-6, CRP, NF-κb and NLRP3, which plays a probiotic function in AS [62–65]. Oscillospira, an anti-inflammatory-related bacteria that can produce SCFAs, which have been shown to improve inflammatory responses and lipid deposition [66,67]. Desulfovibrio is a butyrate-producing opportunistic pathogen that produces endotoxin to disrupt intestinal barrier function and induce inflammatory response [68,69]. Desulfovibrio accelerates the development of AS by increasing the intestinal permeability of Apoe −/− mice, and inhibiting the activation of NF-κb can reduce the atherosclerotic damage induced by Desulfovibrio [70].

As the main signaling molecule of GM - host interaction, GM metabolites are closely related to the pathologic status of AS [71]. The SCFAs are the iconic products of GM with properties of immunomodulation, maintaining the intestinal barrier integrity and suppressing inflammation [72,73]. In our study, we observed Rb1 reversed the low production of acetic acid and propionic acid. Orally delivered propionic acid has been reported to alleviate atherosclerotic damage [74]. Several research demonstrated that acetate and propionate effectively regulate the pathophysiological stages of AS, including improving the inflammation, lipid metabolism and endothelial function [75–77]. Correlation analysis with different GM showed that the probiotics such as Lactobacillus were conspicuously positively correlated with acetic acid, propionic acid and butyric acid, while the pathogenetic GM Desulfovibrio was conspicuously negatively correlated. Therefore, it is reasonable to assume that Rb1 might promote the generation of SCFAs by altering the GM structure, thus playing a protective role in AS.

The Changes of microbiota homeostasis in AS rats were accompanied by alterations in some GM metabolites. Pathway analysis

showed that the Arachidonic acid metabolism and Primary bile acid biosynthesis metabolism pathways were the most disturbed metabolic pathways in the AS model rats. Arachidonic acid is an important polyunsaturated fatty acid in human, which has been shown to mediate a wide range of proinflammatory effects [78]. Studies have confirmed that lipid metabolism disorders can lead to arachidonic acid and its metabolic dysfunction, which can induce an inflammatory response, thus aggravating the development of AS [79,80]. We found that the elevated levels of arachidonic acid metabolites 20-Hydroxyeicosatetraenoic acid and Leukotriene D4 in the AS rats. After the RB1 intervention, these two metabolite levels were substantially decreased in the AS rats, which indicated that RB1 restored the arachidonic acid metabolism disorder. In addition, the mechanism of RB1 in treating AS might also involve the regulation of primary bile acid biosynthesis. Bile acids are a major component of bile, which participates in the pathological process of many metabolic diseases by regulating lipid metabolism [81,82]. In relevant studies, it was found that the level of primary bile acids was conspicuously increased in rats and patients with lipid metabolism disorder [83,84]. Our study arrived at consistent conclusions regarding increased bile acid production. Notably, Previous studies have shown that bile acid can alleviate the progression of AS by improving inflammatory responses, endothelial function and lipid homeostasis [85–87]. Therefore, further studies are needed to reveal the mechanism of RB1 in regulating the metabolic profile of bile acids in AS rats. The correlation analysis of differential metabolites and inflammatory factors indicated that RB1's improvement of inflammation in AS rats might be closely related to its regulation of fecal metabolism profile.

5. Conclusion

In conclusion, this study indicates that Rb1 is effective for treating HFD-induced AS. Rb1 can improve dyslipidemia, endothelial cell damage and inflammation. In addition, Rb1 can regulate the intestinal microecology, including increasing microbial diversity, remodeling the gut microbial composition and promoting the production of SCFAs. Untargeted fecal metabolomics indicated that Rb1 significantly modulates HFD-induced dysregulation of arachidonic acid metabolism and Primary bile acid biosynthesis. The improvement of inflammatory response, fecal SCFAs profile and metabolite profile further supported the favorable regulation of GM. Our research provides an experimental and theoretical support for exploring the treatment effect of Rb1. Future experiments should focus on the specific mechanism by which GM influences endogenous metabolites to treat AS.

Ethics approval

The animal study protocol was approved by the Animal Ethics Committee of Heilongjiang University of Chinese Medicine (No. 2022062023).

Funding statement

This research was supported by the Natural Science Foundation of Heilongjiang Province (ZD2020H006).

Data availability statement

The raw sequence reads 16S rRNA sequencing analysis are available in NCBI Sequence Read Archive with the accession number (PRJNA950603). Other datasets used and/or analyzed during the current study are available from the corresponding author on reasonable request.

CRediT authorship contribution statement

Yuqin Liang: Writing – review & editing, Writing – original draft, Investigation, Data curation, Conceptualization. **Jiaqi Fu:** Writing – review & editing, Software, Investigation. **Yunhe Shi:** Software, Investigation, Formal analysis, Data curation. **Xin Jiang:** Methodology, Investigation, Data curation. **Fang Lu:** Supervision, Resources, Methodology, Formal analysis. **Shumin Liu:** Writing – review & editing, Supervision, Funding acquisition, Conceptualization.

Declaration of competing interest

The authors declare that they have no known competing financial interests or personal relationships that could have appeared to influence the work reported in this paper.

Acknowledgements

Not applicable.

Appendix A. Supplementary data

Supplementary data to this article can be found online at https://doi.org/10.1016/j.heliyon.2024.e27597.

References

[1] J. Most, V. Tosti, L.M. Redman, L. Fontana, Calorie restriction in humans: an update, Ageing Res. Rev. 39 (2017) 36–45, https://doi.org/10.1016/j.arr.2016.08.005.
[2] J.L.M. Björkegren, A.J. Lusis, Atherosclerosis: Recent developments, Cell 185 (2022) 1630–1645, https://doi.org/10.1016/j.cell.2022.04.004.
[3] P. Libby, P.M. Ridker, G.K. Hansson, Progress and challenges in translating the biology of atherosclerosis, Nature 473 (2011) 317–325, https://doi.org/10.1038/nature10146.
[4] P. Libby, The changing landscape of atherosclerosis, Nature 592 (2021) 524–533, https://doi.org/10.1038/s41586-021-03392-8.
[5] A. Poznyak, A.V. Grechko, P. Poggio, V.A. Myasoedova, V. Alfieri, A.N. Orekhov, The diabetes mellitus-atherosclerosis Connection: the role of lipid and glucose metabolism and chronic inflammation, Int. J. Mol. Sci. 21 (2020) 1835, https://doi.org/10.3390/ijms21051835.
[6] S.E. Engelen, A.J.B. Robinson, Y.-X. Zurke, C. Monaco, Therapeutic strategies targeting inflammation and immunity in atherosclerosis: how to proceed? Nat. Rev. Cardiol. 19 (2022) 522–542, https://doi.org/10.1038/s41569-021-00668-4.
[7] A. Koh, F. De Vadder, P. Kovatcheva-Datchary, F. Bäckhed, From dietary fiber to host Physiology: short-chain fatty acids as key bacterial metabolites, Cell 165 (2016) 1332–1345, https://doi.org/10.1016/j.cell.2016.05.041.
[8] C.L. Boulangé, A.L. Neves, J. Chilloux, J.K. Nicholson, M.-E. Dumas, Impact of the gut microbiota on inflammation, obesity, and metabolic disease, Genome Med. 8 (2016) 42, https://doi.org/10.1186/s13073-016-0303-2.
[9] O.O. Erejuwa, S.A. Sulaiman, M.S. Ab Wahab, Modulation of gut microbiota in the management of metabolic disorders: the prospects and challenges, Int. J. Mol. Sci. 15 (2014) 4158–4188, https://doi.org/10.3390/ijms15034158.
[10] Y. Zou, X. Song, N. Liu, W. Sun, B. Liu, Intestinal flora: a potential new regulator of cardiovascular disease, Aging Dis 13 (2022) 753–772, https://doi.org/10.14336/AD.2021.1022.
[11] W.H.W. Tang, T. Kitai, S.L. Hazen, Gut microbiota in cardiovascular health and disease, Circ. Res. 120 (2017) 1183–1196, https://doi.org/10.1161/CIRCRESAHA.117.309715.
[12] Q. Zhang, L. Zhang, C. Chen, P. Li, B. Lu, The gut microbiota-artery axis: a bridge between dietary lipids and atherosclerosis? Prog. Lipid Res. 89 (2023) 101209 https://doi.org/10.1016/j.plipres.2022.101209.
[13] A.L. Jonsson, F. Bäckhed, Role of gut microbiota in atherosclerosis, Nat. Rev. Cardiol. 14 (2017) 79–87, https://doi.org/10.1038/nrcardio.2016.183.
[14] M. Vourakis, G. Mayer, G. Rousseau, The role of gut microbiota on cholesterol metabolism in atherosclerosis, Int. J. Mol. Sci. 22 (2021) 8074, https://doi.org/10.3390/ijms22158074.
[15] E. Sanchez-Rodriguez, A. Egea-Zorrilla, J. Plaza-Díaz, J. Aragón-Vela, S. Muñoz-Quezada, L. Tercedor-Sánchez, F. Abadia-Molina, The gut microbiota and its Implication in the development of atherosclerosis and related cardiovascular diseases, Nutrients 12 (2020) 605, https://doi.org/10.3390/nu12030605.
[16] J. Yao, Y. Chen, M. Xu, The critical role of short-chain fatty acids in health and disease: a subtle focus on cardiovascular disease-NLRP3 inflammasome-angiogenesis axis, Clin. Immunol. 238 (2022) 109013, https://doi.org/10.1016/j.clim.2022.109013.
[17] T. Hu, Q. Wu, Q. Yao, K. Jiang, J. Yu, Q. Tang, Short-chain fatty acid metabolism and multiple effects on cardiovascular diseases, Ageing Res. Rev. 81 (2022) 101706, https://doi.org/10.1016/j.arr.2022.101706.
[18] B. Deng, L. Tao, Y. Wang, Natural products against inflammation and atherosclerosis: targeting on gut microbiota, Front. Microbiol. 13 (2022) 997056, https://doi.org/10.3389/fmicb.2022.997056.
[19] H. Liu, L. Zhu, L. Chen, L. Li, Therapeutic potential of traditional Chinese medicine in atherosclerosis: a review, Phytother Res. 36 (2022) 4080–4100, https://doi.org/10.1002/ptr.7590.
[20] L. Qin, J. Wang, R. Zhao, X. Zhang, Y. Mei, Ginsenoside-Rb1 improved diabetic Cardiomyopathy through regulating calcium signaling by alleviating protein O-GlcNAcylation, J. Agric. Food Chem. 67 (2019) 14074–14085, https://doi.org/10.1021/acs.jafc.9b05706.
[21] P. Zhou, W. Xie, S. He, Y. Sun, X. Meng, G. Sun, X. Sun, Ginsenoside Rb1 as an anti-Diabetic agent and its Underlying mechanism analysis, Cells 8 (2019) 204, https://doi.org/10.3390/cells8030204.
[22] Z. Jiang, Y. Wang, X. Zhang, T. Peng, Y. Lu, J. Leng, Q. Xie, Preventive and therapeutic effects of ginsenoside Rb1 for neural injury during cerebral infarction in rats, Am. J. Chin. Med. 41 (2013) 341–352, https://doi.org/10.1142/S0192415X13500250.
[23] P. Zhou, W. Xie, Y. Luo, S. Lu, Z. Dai, R. Wang, X. Zhang, G. Li, G. Sun, X. Sun, Inhibitory effects of ginsenoside Rb1 on early atherosclerosis in ApoE-/- mice via inhibition of apoptosis and enhancing autophagy, Molecules 23 (2018) 2912, https://doi.org/10.3390/molecules23112912.
[24] Z.-C. Wang, K.-M. Niu, Y.-J. Wu, K.-R. Du, L.-W. Qi, Y.-B. Zhou, H.-J. Sun, A dual Keap1 and p47phox inhibitor Ginsenoside Rb1 ameliorates high glucose/ox-LDL-induced endothelial cell injury and atherosclerosis, Cell Death Dis. 13 (2022) 824, https://doi.org/10.1038/s41419-022-05274-x.
[25] Q.-Y. Li, L. Chen, W.-H. Fu, Z.-D. Li, B. Wang, X.-J. Shi, M.-K. Zhong, Ginsenoside Rb1 inhibits proliferation and inflammatory responses in rat aortic smooth muscle cells, J. Agric. Food Chem. 59 (2011) 6312–6318, https://doi.org/10.1021/jf200424k.
[26] S. Zhang, J. Deng, Y. Gao, D. Yang, Q. Gong, X. Huang, Ginsenoside Rb_1 inhibits the carotid neointimal hyperplasia induced by balloon injury in rats via suppressing the phenotype modulation of vascular smooth muscle cells, Eur. J. Pharmacol. 685 (2012) 126–132, https://doi.org/10.1016/j.ejphar.2012.04.032.
[27] P. Zhou, X. Zhang, M. Guo, R. Guo, L. Wang, Z. Zhang, Z. Lin, M. Dong, H. Dai, X. Ji, H. Lu, Ginsenoside Rb1 ameliorates CKD-associated vascular calcification by inhibiting the Wnt/β-catenin pathway, J. Cell Mol. Med. 23 (2019) 7088–7098, https://doi.org/10.1111/jcmm.14611.
[28] Y. Liu, C. Dou, G. Wei, L. Zhang, W. Xiong, L. Wen, C. Xiang, C. Chen, T. Zhang, A. Altamirano, Y. Chen, T.-E. Zhang, Z. Yan, Usnea improves high-fat diet- and vitamin D3-induced atherosclerosis in rats by remodeling intestinal flora homeostasis, Front. Pharmacol. 13 (2022) 1064872, https://doi.org/10.3389/fphar.2022.1064872.
[29] J. Yan, Y. Pan, W. Shao, C. Wang, R. Wang, Y. He, M. Zhang, Y. Wang, T. Li, Z. Wang, W. Liu, Z. Wang, X. Sun, S. Dong, Beneficial effect of the short-chain fatty acid propionate on vascular calcification through intestinal microbiota remodelling, Microbiome 10 (2022) 195, https://doi.org/10.1186/s40168-022-01390-0.
[30] A. Grebe, F. Hoss, E. Latz, NLRP3 inflammasome and the IL-1 pathway in atherosclerosis, Circ. Res. 122 (2018) 1722–1740, https://doi.org/10.1161/CIRCRESAHA.118.311362.
[31] E. Brandsma, N.J. Kloosterhuis, M. Koster, D.C. Dekker, M.J.J. Gijbels, S. van der Velden, M. Ríos-Morales, M.J.R. van Faassen, M.G. Loreti, A. de Bruin, J. Fu, F. Kuipers, B.M. Bakker, M. Westerterp, M.P.J. de Winther, M.H. Hofker, B. van de Sluis, D.P.Y. Koonen, A proinflammatory gut microbiota increases systemic inflammation and accelerates atherosclerosis, Circ. Res. 124 (2019) 94–100, https://doi.org/10.1161/CIRCRESAHA.118.313234.
[32] J. Xu, M. Kitada, Y. Ogura, D. Koya, Relationship between autophagy and metabolic Syndrome characteristics in the pathogenesis of atherosclerosis, Front. Cell Dev. Biol. 9 (2021) 641852, https://doi.org/10.3389/fcell.2021.641852.
[33] Y. Lu, X. Cui, L. Zhang, X. Wang, Y. Xu, Z. Qin, G. Liu, Q. Wang, K. Tian, K.S. Lim, C.J. Charles, J. Zhang, J. Tang, The functional role of lipoproteins in atherosclerosis: novel directions for diagnosis and targeting therapy, Aging Dis 13 (2022) 491–520, https://doi.org/10.14336/AD.2021.0929.
[34] F. Gao, J. Chen, H. Zhu, A potential strategy for treating atherosclerosis: improving endothelial function via AMP-activated protein kinase, Sci. China Life Sci. 61 (2018) 1024–1029, https://doi.org/10.1007/s11427-017-9285-1.
[35] Y. Zhao, Y. Yang, R. Xing, X. Cui, Y. Xiao, L. Xie, P. You, T. Wang, L. Zeng, W. Peng, D. Li, H. Chen, M. Liu, Hyperlipidemia induces typical atherosclerosis development in Ldlr and Apoe deficient rats, Atherosclerosis 271 (2018) 26–35, https://doi.org/10.1016/j.atherosclerosis.2018.02.015.
[36] D. Wolf, K. Ley, Immunity and inflammation in atherosclerosis, Circ. Res. 124 (2019) 315–327, https://doi.org/10.1161/CIRCRESAHA.118.313591.
[37] M. Bäck, A. Yurdagul, I. Tabas, K. Öörni, P.T. Kovanen, Inflammation and its resolution in atherosclerosis: mediators and therapeutic opportunities, Nat. Rev. Cardiol. 16 (2019) 389–406, https://doi.org/10.1038/s41569-019-0169-2.
[38] A.C. Doran, Inflammation resolution: implications for atherosclerosis, Circ. Res. 130 (2022) 130–148, https://doi.org/10.1161/CIRCRESAHA.121.319822.
[39] Y. Zhu, X. Xian, Z. Wang, Y. Bi, Q. Chen, X. Han, D. Tang, R. Chen, Research progress on the relationship between atherosclerosis and inflammation, Biomolecules 8 (2018) 80, https://doi.org/10.3390/biom8030080.
[40] G. Du, Y. Song, T. Zhang, L. Ma, N. Bian, X. Chen, J. Feng, Q. Chang, Z. Li, Simvastatin attenuates TNF-α-induced apoptosis in endothelial progenitor cells via the upregulation of SIRT1, Int. J. Mol. Med. 34 (2014) 177–182, https://doi.org/10.3892/ijmm.2014.1740.

[41] D.-H. Kim, C.A. Meza, H. Clarke, J.-S. Kim, R.C. Hickner, Vitamin D and endothelial function, Nutrients 12 (2020) 575, https://doi.org/10.3390/nu12020575.
[42] A. Virdis, R. Colucci, N. Bernardini, C. Blandizzi, S. Taddei, S. Masi, Microvascular endothelial dysfunction in human obesity: role of TNF-α, J. Clin. Endocrinol. Metab. 104 (2019) 341–348, https://doi.org/10.1210/jc.2018-00512.
[43] S.Y. Eun, Y.S. Ko, S.W. Park, K.C. Chang, H.J. Kim, IL-1β enhances vascular smooth muscle cell proliferation and migration via P2Y2 receptor-mediated RAGE expression and HMGB1 release, Vasc. Pharmacol. 72 (2015) 108–117, https://doi.org/10.1016/j.vph.2015.04.013.
[44] M. Liu, M. Yan, H. Lv, B. Wang, X. Lv, H. Zhang, S. Xiang, J. Du, T. Liu, Y. Tian, X. Zhang, F. Zhou, T. Cheng, Y. Zhu, H. Jiang, Y. Cao, D. Ai, Macrophage K63-linked ubiquitination of YAP promotes its nuclear localization and exacerbates atherosclerosis, Cell Rep. 32 (2020) 107990, https://doi.org/10.1016/j.celrep.2020.107990.
[45] M. Tayefi, M. Tajfard, S. Saffar, P. Hanachi, A.R. Amirabadizadeh, H. Esmaeily, A. Taghipour, G.A. Ferns, M. Moohebati, M. Ghayour-Mobarhan, hs-CRP is strongly associated with coronary heart disease (CHD): a data mining approach using decision tree algorithm, Comput. Methods Progr. Biomed. 141 (2017) 105–109, https://doi.org/10.1016/j.cmpb.2017.02.001.
[46] D. Karunakaran, M.-A. Nguyen, M. Geoffrion, D. Vreeken, Z. Lister, H.S. Cheng, N. Otte, P. Essebier, H. Wyatt, J.W. Kandiah, R. Jung, F.J. Alenghat, A. Mompeon, R. Lee, C. Pan, E. Gordon, A. Rasheed, A.J. Lusis, P. Liu, L.P. Matic, U. Hedin, J.E. Fish, L. Guo, F. Kolodgie, R. Virmani, J.M. van Gils, K.J. Rayner, RIPK1 expression associates with inflammation in early atherosclerosis in humans and can Be therapeutically silenced to reduce NF-κB activation and atherogenesis in mice, Circulation 143 (2021) 163–177, https://doi.org/10.1161/CIRCULATIONAHA.118.038379.
[47] W. Li, K. Jin, J. Luo, W. Xu, Y. Wu, J. Zhou, Y. Wang, R. Xu, L. Jiao, T. Wang, G. Yang, NF-κB and its crosstalk with endoplasmic reticulum stress in atherosclerosis, Front Cardiovasc Med 9 (2022) 988266, https://doi.org/10.3389/fcvm.2022.988266.
[48] B.R. Sharma, T.-D. Kanneganti, NLRP3 inflammasome in cancer and metabolic diseases, Nat. Immunol. 22 (2021) 550–559, https://doi.org/10.1038/s41590-021-00886-5.
[49] C. Guo, S. Xie, Z. Chi, J. Zhang, Y. Liu, L. Zhang, M. Zheng, X. Zhang, D. Xia, Y. Ke, L. Lu, D. Wang, Bile acids control inflammation and metabolic disorder through inhibition of NLRP3 inflammasome, Immunity 45 (2016) 802–816, https://doi.org/10.1016/j.immuni.2016.09.008.
[50] I.S. Afonina, Z. Zhong, M. Karin, R. Beyaert, Limiting inflammation-the negative regulation of NF-κB and the NLRP3 inflammasome, Nat. Immunol. 18 (2017) 861–869, https://doi.org/10.1038/ni.3772.
[51] E.-K. Jo, J.K. Kim, D.-M. Shin, C. Sasakawa, Molecular mechanisms regulating NLRP3 inflammasome activation, Cell. Mol. Immunol. 13 (2016) 148–159, https://doi.org/10.1038/cmi.2015.95.
[52] F. Bian, X.-Y. Yang, G. Xu, T. Zheng, S. Jin, CRP-induced NLRP3 inflammasome activation increases LDL transcytosis across endothelial cells, Front. Pharmacol. 10 (2019) 40, https://doi.org/10.3389/fphar.2019.00040.
[53] W. Chen, S. Zhang, J. Wu, T. Ye, S. Wang, P. Wang, D. Xing, Butyrate-producing bacteria and the gut-heart axis in atherosclerosis, Clin. Chim. Acta 507 (2020) 236–241, https://doi.org/10.1016/j.cca.2020.04.037.
[54] L. Anto, C.N. Blesso, Interplay between diet, the gut microbiome, and atherosclerosis: role of dysbiosis and microbial metabolites on inflammation and disordered lipid metabolism, J. Nutr. Biochem. 105 (2022) 108991, https://doi.org/10.1016/j.jnutbio.2022.108991.
[55] K. Kasahara, T. Tanoue, T. Yamashita, K. Yodoi, T. Matsumoto, T. Emoto, T. Mizoguchi, T. Hayashi, N. Kitano, N. Sasaki, K. Atarashi, K. Honda, K.-I. Hirata, Commensal bacteria at the crossroad between cholesterol homeostasis and chronic inflammation in atherosclerosis, J. Lipid Res. 58 (2017) 519–528, https://doi.org/10.1194/jlr.M072165.
[56] A. Wang, B. Guan, C. Shao, L. Zhao, Q. Li, H. Hao, Z. Gao, K. Chen, Y. Hou, H. Xu, Qing-Xin-Jie-Yu Granule alleviates atherosclerosis by reshaping gut microbiota and metabolic homeostasis of ApoE-/- mice, Phytomedicine 103 (2022) 154220, https://doi.org/10.1016/j.phymed.2022.154220.
[57] G. Shi, Y. Lin, Y. Wu, J. Zhou, L. Cao, J. Chen, Y. Li, N. Tan, S. Zhong, Bacteroides fragilis supplementation deteriorated metabolic dysfunction, inflammation, and aorta atherosclerosis by inducing gut microbiota dysbiosis in animal model, Nutrients 14 (2022) 2199, https://doi.org/10.3390/nu14112199.
[58] J. Li, S. Lin, P.M. Vanhoutte, C.W. Woo, A. Xu, Akkermansia muciniphila protects against atherosclerosis by preventing metabolic endotoxemia-induced inflammation in Apoe-/- mice, Circulation 133 (2016) 2434–2446, https://doi.org/10.1161/CIRCULATIONAHA.115.019645.
[59] M. Jin, L. Zheng, Y. Wei, J. Cheng, D. Zhang, S. Yan, H. Qin, Q. Wang, X. Ci, H. Feng, Enterobacter cloacae aggravates metabolic disease by inducing inflammation and lipid accumulation, Environ. Toxicol. Pharmacol. 90 (2022) 103819, https://doi.org/10.1016/j.etap.2022.103819.
[60] L. Khalili, A.M. Centner, G. Salazar, Effects of berries, phytochemicals, and probiotics on atherosclerosis through gut microbiota modification: a meta-analysis of animal studies, Int. J. Mol. Sci. 24 (2023) 3084, https://doi.org/10.3390/ijms24043084.
[61] I.C.L. van den Munckhof, A. Kurilshikov, R. Ter Horst, N.P. Riksen, L.a.B. Joosten, A. Zhernakova, J. Fu, S.T. Keating, M.G. Netea, J. de Graaf, J.H.W. Rutten, Role of gut microbiota in chronic low-grade inflammation as potential driver for atherosclerotic cardiovascular disease: a systematic review of human studies, Obes. Rev. 19 (2018) 1719–1734, https://doi.org/10.1111/obr.12750.
[62] M.J. Claesson, I.B. Jeffery, S. Conde, S.E. Power, E.M. O'Connor, S. Cusack, H.M.B. Harris, M. Coakley, B. Lakshminarayanan, O. O'Sullivan, G.F. Fitzgerald, J. Deane, M. O'Connor, N. Harnedy, K. O'Connor, D. O'Mahony, D. van Sinderen, M. Wallace, L. Brennan, C. Stanton, J.R. Marchesi, A.P. Fitzgerald, F. Shanahan, C. Hill, R.P. Ross, P.W. O'Toole, Gut microbiota composition correlates with diet and health in the elderly, Nature 488 (2012) 178–184, https://doi.org/10.1038/nature11319.
[63] Z. Jie, H. Xia, S.-L. Zhong, Q. Feng, S. Li, S. Liang, H. Zhong, Z. Liu, Y. Gao, H. Zhao, D. Zhang, Z. Su, Z. Fang, Z. Lan, J. Li, L. Xiao, J. Li, R. Li, X. Li, F. Li, H. Ren, Y. Huang, Y. Peng, G. Li, B. Wen, B. Dong, J.-Y. Chen, Q.-S. Geng, Z.-W. Zhang, H. Yang, J. Wang, J. Wang, X. Zhang, L. Madsen, S. Brix, G. Ning, X. Xu, X. Liu, Y. Hou, H. Jia, K. He, K. Kristiansen, The gut microbiome in atherosclerotic cardiovascular disease, Nat. Commun. 8 (2017) 845, https://doi.org/10.1038/s41467-017-00900-1.
[64] Q. Wang, Y. He, X. Li, T. Zhang, M. Liang, G. Wang, J. Zhao, H. Zhang, W. Chen, Lactobacillus reuteri CCFM8631 alleviates hypercholesterolaemia caused by the paigen atherogenic diet by regulating the gut microbiota, Nutrients 14 (2022) 1272, https://doi.org/10.3390/nu14061272.
[65] X.-N. Zhang, Z.-L. Yu, J.-Y. Chen, X.-Y. Li, Z.-P. Wang, M. Wu, L.-T. Liu, The crosstalk between NLRP3 inflammasome and gut microbiome in atherosclerosis, Pharmacol. Res. 181 (2022) 106289, https://doi.org/10.1016/j.phrs.2022.106289.
[66] U. Gophna, T. Konikoff, H.B. Nielsen, Oscillospira and related bacteria - from metagenomic species to metabolic features, Environ. Microbiol. 19 (2017) 835–841, https://doi.org/10.1111/1462-2920.13658.
[67] R. Sun, H. Niu, M. Sun, X. Miao, X. Jin, X. Xu, C. Yanping, H. Mei, J. Wang, L. Da, Y. Su, Effects of Bacillus subtilis natto JLCC513 on gut microbiota and intestinal barrier function in obese rats, J. Appl. Microbiol. 133 (2022) 3634–3644, https://doi.org/10.1111/jam.15797.
[68] W.-C. Huang, C.-L. Tung, Y.-C.S.H. Yang, I.-H. Lin, X.E. Ng, Y.-T. Tung, Endurance exercise ameliorates Western diet-induced atherosclerosis through modulation of microbiota and its metabolites, Sci. Rep. 12 (2022) 3612, https://doi.org/10.1038/s41598-022-07317-x.
[69] Y. Nie, X.-Q. Xie, L. Zhou, Q. Guan, Y. Ren, Y. Mao, J.-S. Shi, Z.-H. Xu, Y. Geng, Desulfovibrio fairfieldensis-derived outer membrane vesicles damage epithelial barrier and induce inflammation and pyroptosis in macrophages, Cells 12 (2022) 89, https://doi.org/10.3390/cells12010089.
[70] K. Zhang, X. Qin, J. Qiu, T. Sun, K. Qu, A.U. Din, W. Yan, T. Li, Y. Chen, W. Gu, X. Rao, G. Wang, Desulfovibrio desulfuricans aggravates atherosclerosis by enhancing intestinal permeability and endothelial TLR4/NF-κB pathway in Apoe -/- mice, Genes Dis 10 (2023) 239–253, https://doi.org/10.1016/j.gendis.2021.09.007.
[71] H. Cao, Y. Zhu, G. Hu, Q. Zhang, L. Zheng, Gut microbiome and metabolites, the future direction of diagnosis and treatment of atherosclerosis? Pharmacol. Res. 187 (2023) 106586 https://doi.org/10.1016/j.phrs.2022.106586.
[72] B. Dalile, L. Van Oudenhove, B. Vervliet, K. Verbeke, The role of short-chain fatty acids in microbiota-gut-brain communication, Nat. Rev. Gastroenterol. Hepatol. 16 (2019) 461–478, https://doi.org/10.1038/s41575-019-0157-3.
[73] P. Liu, Y. Wang, G. Yang, Q. Zhang, L. Meng, Y. Xin, X. Jiang, The role of short-chain fatty acids in intestinal barrier function, inflammation, oxidative stress, and colonic carcinogenesis, Pharmacol. Res. 165 (2021) 105420, https://doi.org/10.1016/j.phrs.2021.105420.
[74] H. Bartolomaeus, A. Balogh, M. Yakoub, S. Homann, L. Markó, S. Höges, D. Tsvetkov, A. Krannich, S. Wundersitz, E.G. Avery, N. Haase, K. Kräker, L. Hering, M. Maase, K. Kusche-Vihrog, M. Grandoch, J. Fielitz, S. Kempa, M. Gollasch, Z. Zhumadilov, S. Kozhakhmetov, A. Kushugulova, K.-U. Eckardt, R. Dechend, L.

C. Rump, S.K. Forslund, D.N. Müller, J. Stegbauer, N. Wilck, Short-chain fatty acid propionate protects from hypertensive cardiovascular damage, Circulation 139 (2019) 1407–1421, https://doi.org/10.1161/CIRCULATIONAHA.118.036652.

[75] J. He, P. Zhang, L. Shen, L. Niu, Y. Tan, L. Chen, Y. Zhao, L. Bai, X. Hao, X. Li, S. Zhang, L. Zhu, Short-chain fatty acids and their association with signalling pathways in inflammation, glucose and lipid metabolism, Int. J. Mol. Sci. 21 (2020) 6356, https://doi.org/10.3390/ijms21176356.

[76] T. Liu, J. Li, Y. Liu, N. Xiao, H. Suo, K. Xie, C. Yang, C. Wu, Short-chain fatty acids suppress lipopolysaccharide-induced production of nitric oxide and proinflammatory cytokines through inhibition of NF-κB pathway in RAW264.7 cells, Inflammation 35 (2012) 1676–1684, https://doi.org/10.1007/s10753-012-9484-z.

[77] K. Stø, J. Valeur, T. Ueland, G.H. Malmstrøm, V. Bjerkeli, M. Trøseid, J.R. Hov, K. Holm, B. Vestad, B. Halvorsen, M. Skjelland, K.R. Skagen, Fecal level of butyric acid, a microbiome-derived metabolite, is increased in patients with severe carotid atherosclerosis, Sci. Rep. 12 (2022) 22378, https://doi.org/10.1038/s41598-022-26759-x.

[78] T. Yagami, Y. Yamamoto, H. Koma, Physiological and pathological roles of 15-deoxy-δ12,14-prostaglandin J2 in the central nervous system and neurological diseases, Mol. Neurobiol. 55 (2018) 2227–2248, https://doi.org/10.1007/s12035-017-0435-4.

[79] Y. Sun, D. Wu, W. Zeng, Y. Chen, M. Guo, B. Lu, H. Li, C. Sun, L. Yang, X. Jiang, Q. Gao, The role of intestinal dysbacteriosis induced arachidonic acid metabolism disorder in inflammaging in atherosclerosis, Front. Cell. Infect. Microbiol. 11 (2021) 618265, https://doi.org/10.3389/fcimb.2021.618265.

[80] S.-S. Xu, X.-L. Zhang, S.-S. Liu, S.-T. Feng, G.-M. Xiang, C.-J. Xu, Z.-Y. Fan, K. Xu, N. Wang, Y. Wang, J.-J. Che, Z.-G. Liu, Y.-L. Mu, K. Li, Multi-omic analysis in a metabolic syndrome porcine model implicates arachidonic acid metabolism disorder as a risk factor for atherosclerosis, Front. Nutr. 9 (2022) 807118, https://doi.org/10.3389/fnut.2022.807118.

[81] A. Kumari, D. Pal Pathak, S. Asthana, Bile acids mediated potential functional interaction between FXR and FATP5 in the regulation of Lipid Metabolism, Int. J. Biol. Sci. 16 (2020) 2308–2322, https://doi.org/10.7150/ijbs.44774.

[82] E. Kwong, Y. Li, P.B. Hylemon, H. Zhou, Bile acids and sphingosine-1-phosphate receptor 2 in hepatic lipid metabolism, Acta Pharm. Sin. B 5 (2015) 151–157, https://doi.org/10.1016/j.apsb.2014.12.009.

[83] B.C. Ferslew, G. Xie, C.K. Johnston, M. Su, P.W. Stewart, W. Jia, K.L.R. Brouwer, A.S. Barritt, Altered bile acid metabolome in patients with nonalcoholic steatohepatitis, Dig. Dis. Sci. 60 (2015) 3318–3328, https://doi.org/10.1007/s10620-015-3776-8.

[84] N. Jiao, S.S. Baker, A. Chapa-Rodriguez, W. Liu, C.A. Nugent, M. Tsompana, L. Mastrandrea, M.J. Buck, R.D. Baker, R.J. Genco, R. Zhu, L. Zhu, Suppressed hepatic bile acid signalling despite elevated production of primary and secondary bile acids in NAFLD, Gut 67 (2018) 1881–1891, https://doi.org/10.1136/gutjnl-2017-314307.

[85] J.-Y. Yang, T.-T. Zhang, Z.-L. Yu, X.-Y. Li, Y.-C. Zhao, X.-Z. Mao, Y.-M. Wang, C.-H. Xue, Phosphatidylglucose alleviates atherosclerosis by increasing cholesterol alienation to bile acids and cholesterol efflux in ApoE-/- mice, J. Sci. Food Agric. 103 (2023) 5529–5538, https://doi.org/10.1002/jsfa.12626.

[86] F. Wang, C. Zhao, G. Tian, X. Wei, Z. Ma, J. Cui, R. Wei, Y. Bao, W. Kong, J. Zheng, Naringin alleviates atherosclerosis in ApoE-/- mice by regulating cholesterol metabolism involved in gut microbiota remodeling, J. Agric. Food Chem. 68 (2020) 12651–12660, https://doi.org/10.1021/acs.jafc.0c05800.

[87] R. Bao, W. Wang, B. Chen, J. Pan, Q. Chen, M. Liu, D. Wang, Y. Wu, H. Yu, L. Han, Y. Zhang, T. Wang, Dioscin ameliorates hyperuricemia-induced atherosclerosis by modulating of cholesterol metabolism through FXR-signaling pathway, Nutrients 14 (2022) 1983, https://doi.org/10.3390/nu14091983.